Cancer Research

Tissue Stiffness and Hypoxia Modulate the Integrin-Linked Kinase ILK to Control Breast Cancer Stem-like Cells

Mei-Fong Pang[1,2], Michael J. Siedlik[1], Siyang Han[2], Melody Stallings-Mann[3], Derek C. Radisky[3], and Celeste M. Nelson[1,2]

Abstract

Breast tumors are stiffer and more hypoxic than nonmalignant breast tissue. Here we report that stiff and hypoxic microenvironments promote the development of breast cancer stem-like cells (CSC) through modulation of the integrin-linked kinase ILK. Depleting ILK blocked stiffness and hypoxia-dependent acquisition of CSC marker expression and behavior, whereas ectopic expression of ILK stimulated CSC development under softer or normoxic conditions. Stiff microenvironments also promoted tumor formation and metastasis *in ovo*, where depleting ILK significantly abrogated the tumorigenic and metastatic potential of invasive breast cancer cells. We further found that the ILK-mediated phenotypes induced by stiff and hypoxic microenvironments are regulated by PI3K/Akt. Analysis of human breast cancer specimens revealed an association between substratum stiffness, ILK, and CSC markers, insofar as ILK and CD44 were expressed in cancer cells located in tumor regions predicted to be stiff. Our results define ILK as a key mechanotransducer in modulating breast CSC development in response to tissue mechanics and oxygen tension. *Cancer Res; 76(18); 1–11. ©2016 AACR.*

Introduction

The mechanical stiffness of the cellular microenvironment, dominated by the composition and crosslinking of the extracellular matrix (ECM), is a key modulator of cell fate (1, 2). For example, human mesenchymal stem cells differentiate down distinct lineages depending on the stiffness of their underlying substratum (1, 3), and matrix stiffness regulates epithelial plasticity by controlling the induction of epithelial–mesenchymal transition (4). Increased matrix stiffness enhances tumor cell invasiveness and dissemination (5, 6), and can direct the transformation of mammary epithelial cells (7). In contrast, tumors grown in mice with disorganized, compliant ECM architecture are minimally invasive (8). Stiff ECM has been found to promote tumor progression through the induction of signaling pathways downstream of integrins and PI3K (9).

In addition to increased stiffness, invasive breast cancers are frequently hypoxic (10). Tumor hypoxia correlates with poor prognosis and decreased survival in breast cancer patients (11, 12). Hypoxia can activate signaling pathways that regulate cancer stem-like cells (CSC; ref. 13), a distinct population of cancer cells with enhanced proliferative and invasive characteristics (14). Under hypoxic conditions, breast cancer cells express CSC-associated markers, including CD44, Nanog, CD49f, and ALDH (15–19). Hypoxic conditions also promote pluripotency and viability of CSC populations (20, 21).

Integrin-linked kinase (ILK) is a crucial mediator of signal transmission from the ECM. ILK interacts with β1-integrin and transmits extracellular signals from the ECM to regulate cellular activities including anchorage-dependent growth and survival, migration, invasion, differentiation, and tumor angiogenesis (22). Elevated expression of ILK has been closely associated with high-grade human tumors (23, 24) and ILK has been shown to activate oncogenic pathways to promote tumor progression (25). However, it remains unclear how the expression of ILK and its downstream signaling are regulated in the stiff, hypoxic microenvironments common to invasive cancers. Because ILK is a critical adaptor used by cancer cells to sense their surrounding microenvironment, we hypothesized that matrix stiffness and hypoxia could affect ILK signaling in breast cancer cells to regulate breast CSC-associated gene expression and cellular behaviors. Here, we used engineered synthetic substrata to recapitulate the mechanical properties of the normal mammary gland as well as that of breast tumors. We investigated how the mechanical properties and oxygen tension in the tumor microenvironment affect the formation of breast CSCs. We found that breast CSC markers are activated synergistically in response to stiff, hypoxic conditions, and that ILK is an essential regulator of breast CSCs.

Materials and Methods

Cell culture and reagents

MDA-MB-231 human breast carcinoma cells and 4T1 murine mammary carcinoma cells were obtained from the ATCC and maintained in DMEM/F12 or RPMI base medium (respectively) that was supplemented with 10% FBS and 1% gentamycin. Both cell lines were authenticated by short tandem repeat

[1]Department of Chemical & Biological Engineering, Princeton University, Princeton, New Jersey. [2]Department of Molecular Biology, Princeton University, Princeton, New Jersey. [3]Department of Cancer Biology, Mayo Clinic Cancer Center, Jacksonville, Florida.

Note: Supplementary data for this article are available at Cancer Research Online (http://cancerres.aacrjournals.org/).

Corresponding Author: Celeste M. Nelson, Princeton University, 303 Hoyt Laboratory, William Street, Princeton, NJ 08544. Phone: 609-258-8851; Fax: 609-258-1247; E-mail: celesten@princeton.edu

doi: 10.1158/0008-5472.CAN-16-0579

genotyping, tested for mycoplasma contamination (DDC Medical), and were used before passage 20 and within 6 months after resuscitation. To reduce the expression of ILK, cells were transduced with lentiviral particles carrying short hairpin RNA (shRNA) against *ILK* (sc-35667-V and sc-35666-V, Santa Cruz Biotechnology) or control lentivirus expressing a scrambled shRNA sequence. Stable shRNA-expressing clones were produced according to the manufacturer's instructions and selected using puromycin. All cells were maintained in a humidified incubator held at 37°C and 5% CO_2.

To investigate the effect of matrix stiffness, cells were cultured on synthetic substrata of different compliances conjugated with fibronectin, which were prepared as described previously (4). Cells were seeded at a density of 500,000 cells/cm^2 on synthetic substrata and cultured for 72 hours at 37°C in either humidified normoxic conditions (95% air and 5% CO_2) or in a modular incubator chamber (Billups-Rothenberg, Inc.) filled with hypoxic gas (94% N_2, 1% O_2, and 5% CO_2).

Quantitative real-time PCR analysis

Total RNA was extracted using TRIzol reagent according to the manufacturer's instructions, followed by cDNA synthesis using the Verso cDNA synthesis kit (Thermo Scientific). Transcript levels were measured by quantitative real-time PCR (qRT-PCR) using a Bio-Rad Mini Opticon instrument and iTaq Universal SYBR Green Supermix (Bio-Rad). Amplification was followed by melting curve analysis to verify the presence of a single PCR product. Primers specific for *GFP*, *ILK*, *ITGB1*, *CD44*, *Nanog*, *CD49f*, *VEGF-A*, and *18S rRNA* are listed in Supplementary Table S1 (Supplementary Information). The expression level of each mRNA was normalized to that of 18S in the same sample.

Time-lapse imaging and cell tracking

Time-lapse imaging was performed using a Nikon Ti-U inverted microscope equipped with a stage top incubator maintained at 37°C in a 5% CO_2, 90% relative humidity atmosphere (Pathology Devices, Inc.). Images were acquired every 30 minutes using a Plan Fluor 10×/0.3 NA air objective (Nikon) and a Hamamatsu Orca-100 camera. Individual GFP-labeled cells were tracked from the aligned image sequences using the "Manual Tracking" plugin in ImageJ.

Immunoblotting analysis

Samples were lysed in radioimmunoprecipitation assay buffer (Pierce Biotechnology) supplemented with a protease inhibitor cocktail (Roche). Equal amounts of total protein were separated by standard electrophoresis using 4–12% gradient NuPage gels (Invitrogen). Proteins were transferred onto nitrocellulose membranes, which were then blocked and incubated overnight with primary antibodies at 4°C. Antibodies used for immunoblotting were: rabbit anti-β1-integrin (1:1,000; Abcam), rabbit anti-ILK (1:1,000; Abcam), rabbit anti-Nanog (1:1,000; Novus Biologicals), mouse anti-CD44 (1:1,000; Novus Biologicals), and rabbit anti-GAPDH (1:1,000; Cell Signaling Technology). After washing, blots were probed with horseradish peroxidase (HRP)-conjugated anti-rabbit or anti-mouse secondary antibodies (1:5,000; Cell Signaling Technology) for 1 hour. Blots were incubated with ECL Plus Western Blotting Detection System (GE Healthcare) for 5 minutes and signals were detected with a FluorChemE Imager (Cell Biosciences, Inc.).

Soft agar assay

Approximately 5,000 cells were resuspended in serum-free DMEM/F12 medium supplemented with 0.35% agar and plated in a 12-well plate that contained a base layer of DMEM/F12 medium supplemented with 0.7% agar. Cells were incubated for 14 days and the culture medium was changed twice per week. At the end of the experiment, colonies were fixed with 4% PFA, washed with PBS, and imaged. Colonies were counted if they were larger than 10 μm in diameter as measured using ImageJ.

Aldefluor assay and flow cytometry

Cells were harvested by trypsinization using Accutase (eBioscience), washed with PBS, and resuspended in flow cytometry staining buffer (eBioscience). Cells were filtered through a 40-μm cell strainer (Corning) to obtain single-cell suspensions. For intracellular staining, cells were fixed and permeabilized using Foxp3 transcription factor staining buffer set (eBioscience) prior to staining. Cells were stained without fixation for cell surface markers. Cells were incubated with the following fluorochrome-conjugated antibodies at 4°C for 45 minutes: CD49f (1:200, clone GoH3; eBioscience), CD44 (1:100, clone IM7; eBioscience), and Nanog (1:100, clone eBioMLC-51; eBioscience). Stained cells were washed twice with flow cytometry buffer (eBioscience). To assess ALDH activity, the ALDEFLUOR fluorescent reagent sytem (Stem Cell Technologies) was used according to the manufacturer's instructions. Stained cells were analyzed using an LSRII flow cytometer (BD Biosciences) and data were analyzed using FlowJo.

Secondary mammosphere formation assay

A single-cell suspension was seeded at a density of 3,000 cells per well into 12-well ultra-low attachment plates (BD Biosciences). Cells were cultured in DMEM/F12 medium containing 20 ng/mL EGF and 20 ng/mL basic fibroblast growth factor, and culture medium was changed twice per week. After 7 days, primary mammospheres were collected and disassociated enzymatically with 0.05% trypsin (Invitrogen) for 5 minutes at 37°C and mechanically by filtering through a 40-μm cell strainer (Corning). Single-cell suspensions were replated onto 12-well ultra-low attachment plates at a density of 1,000 cells per well. After 14 days, secondary mammospheres were transferred to a 12-well plate. Serum-containing medium was added and secondary mammospheres were allowed to attach to the bottom surface of the plate. After 12 hours, cells were fixed with 4% PFA and stained with 0.05% crystal violet. Samples were imaged, analyzed using ImageJ, and mammospheres were counted if they had a diameter larger than 50 μm.

Mechanical testing of collagen gels

The elastic moduli of gels comprising different concentrations of collagen were estimated from unconfined compression experiments, as described previously (26). Briefly, collagen solutions containing 500-nm fluorescent beads were allowed to gel for at least 30 minutes at 37°C within circular polydimethylsiloxane (Sylgard 184) molds. After gelation, the mold was removed and the cylindrical gel was immersed in PBS. Confocal stacks of the gel were acquired before and 1 minute after loading a glass coverslip of known weight to the top of the gel. The thickness of the gel was estimated from the fluorescence signal of the embedded beads and, as a first approximation, the measured change in thickness was used to estimate the elastic modulus of the gel.

Chicken chorioallantoic membrane assay

Chicken chorioallantoic membrane (CAM) assays were performed as described previously (27). Cells were transduced with recombinant adenovirus encoding GFP at an MOI of 100 for 24 hours prior to implantation. GFP-transduced cells were resuspended in neutralized rat tail type I collagen (BD Biosciences) at a density of 300,000 cells per 30-μL pellet. Cell-embedded collagen gels were implanted on the CAM of a chicken embryo at day 7 of incubation. Tumor formation, angiogenesis, and metastasis were scored in live embryos 5 days later using a stereomicroscope. Images were acquired using a Nikon digital camera.

Human breast cancer samples

Breast cancer biopsies were derived from waste surgical material from de-identified patients, and were formalin-fixed and paraffin-embedded, as per approval by the Mayo Clinic Institutional Review Board. Tissue sections were deparaffinized by placing them into three changes of xylene and rehydrated in a graded ethanol series. The rehydrated tissue samples were rinsed in water and sections were subjected to heat antigen retrieval as described by the manufacturer (DAKO). Slices were incubated with each primary antibody for 1 hour at room temperature. Sections were then rinsed with Tris-buffered saline/Triton-X-100 (TBST) wash buffer, and incubated with each secondary antibody for 30 minutes. For fluorescent detection, tissue sections were rinsed 3 times for 5 minutes each with PBS containing 1.43 μmol/L 4′,6-diamidino-2-phenylindole (DAPI; Thermo Fisher Scientific). Sections were rinsed with PBS and coverslips mounted with anti-fade mounting medium (DAKO). Sections stained for collagen I were rinsed with TBST wash buffer, and secondary incubation was with DAKO Envision anti-rabbit, HRP for 15 minutes. Tissue sections were rinsed with TBST wash buffer and then incubated in 3,3′-diaminobenzidine (DAB+; DAKO), and counterstained with modified Schmidt hematoxylin. Each antibody and its corresponding fluorescent secondary antibody used were: ILK1 (rabbit polyclonal, Cell Signaling Technology #3862) detected by Alexa594-conjugated donkey anti-rabbit IgG (Invitrogen, #A21207); CD44 (mouse IgG2A, Abcam #ab6124) detected by Alexa488-conjugated donkey anti-mouse IgG (H+L) (Invitrogen, #A21202). For DAB staining, collagen I (Abcam ab138492) was used.

Whole slide digital images of each breast cancer sample were captured with the Aperio Scanscope AT2 slide scanner (collagen) and the Aperio Scanscope FL slide scanner (fluorescent images) using a 20× objective. Using the digitized images, areas of high and low collagen content were selected and circled. Cell number in each area was determined by manually counting the number of DAPI-positive nuclei. Similarly, double positive cells (488 and 594) were identified and counted in each selected area. Density of double positive cells was calculated as the total number of positively stained cells per total number of cells in each selected area.

Statistical analysis

Data represent mean ± SEM of at least three independent experiments conducted in triplicate. For CAM assays, data represent mean ± SEM with $n = 5$ chicken embryos per group. For patient samples, statistical significance was tested with the Mann–Whitney *U* test; for all others, statistical analysis was conducted using a two-way ANOVA followed by Bonferroni post-test or Student *t* test. $P < 0.05$ was considered to represent a significant difference between conditions.

Results

Substratum stiffness and oxygen tension regulate the expression of β1-integrin and ILK in invasive breast cancer cells

To investigate how ECM compliance affects breast cancer cells, we used synthetic polyacrylamide substrata to mimic the compliance of the microenvironment in the normal mammary gland (Young modulus, $E \sim 130$ Pa, "soft") and in breast tumors ($E \sim 4020$ Pa, "stiff"; ref. 4). On soft substrata, 4T1 mouse mammary carcinoma cells (Fig. 1A) and MDA-MB-231 human breast carcinoma cells (Supplementary Fig. S1) were rounded in morphology. In contrast, both 4T1 and MDA-MB-231 cells displayed an elongated morphology on stiff substrata. Consistent with the expectation that the elongated cell morphology on stiff substrata was associated with increased interactions with the ECM, RT-PCR and immunoblotting revealed increased expression of β1-integrin and ILK in the cells cultured on stiff substrata at the transcript (Fig. 1B and C) and protein (Fig. 1D) levels.

Hypoxia is prevalent in solid tumors and has been shown to activate stem cell–like properties in several cancers, including breast cancer (28). We found that hypoxia also led to an increase in the transcript and protein levels of β1-integrin (Fig. 1B and D) and ILK (Fig. 1C and D) in both 4T1 and MDA-MB-231 cells (Supplementary Fig. S1). A stiff, hypoxic microenvironment induced the highest expression of these markers (Fig. 1B–D and Supplementary Fig. S1). These results suggest that stiff and hypoxic microenvironments potentiate signaling downstream of β1-integrin and ILK in breast cancer cells.

The presence of breast CSCs correlates with metastasis and relapse in breast cancer patients (29). To determine whether the mechanical microenvironment and oxygen tension can regulate breast CSC gene expression, we examined the relative effects of substratum stiffness and hypoxia on the expression of the CSC markers, CD44, Nanog, CD49f, and ALDH. We found that substratum stiffness and hypoxia led to synergistic increases in the levels of each of these markers in both 4T1 and MDA-MB-231 cells (Fig. 1E–H and Supplementary Fig. S1).

ILK has been found to regulate integrin function and cell motility. We evaluated the effect of stiff substrata on cell movement using time-lapse imaging, which revealed that breast cancer cells cultured on stiff substrata were more motile than those cultured on soft substrata (Fig. 1I). Together, these data suggest that the increased stiffness and decreased oxygen tension of the tumor microenvironment enhances integrin signaling and activates CSC marker expression in invasive breast cancer cells.

ILK and CD44 are elevated in potentially stiff regions of human tumors

To evaluate the relationship between stiffness, ILK expression, and CSC marker induction *in vivo*, we examined the expression of ILK and CD44 in human breast cancer samples. We compared these to relative collagen content, which is highly correlated with stiffness in mammary cancers (30, 31). Immunofluorescence analysis revealed that most tumor cells expressed low levels of ILK and were CD44-negative

in regions of the tumors that contained low levels of collagen (col^{lo}), whereas ILK and CD44 double-positive tumor cells were found in regions that contained high levels of collagen (col^{hi}) (Fig. 1J). In col^{hi} regions, more than 25% of the cells expressed both ILK and CD44. In contrast, only approximately 4% of the cells expressed both markers in col^{lo} regions (Fig. 1K). These data are consistent with the results of our cell culture experiments, and suggest that breast CSCs are preferentially located in stiff microenvironments.

Depleting ILK prevents CSC development in cells on stiff substrata

β1-integrin transmits cues from the ECM through ILK to control cellular behavior (22), and enhanced signaling through ILK has

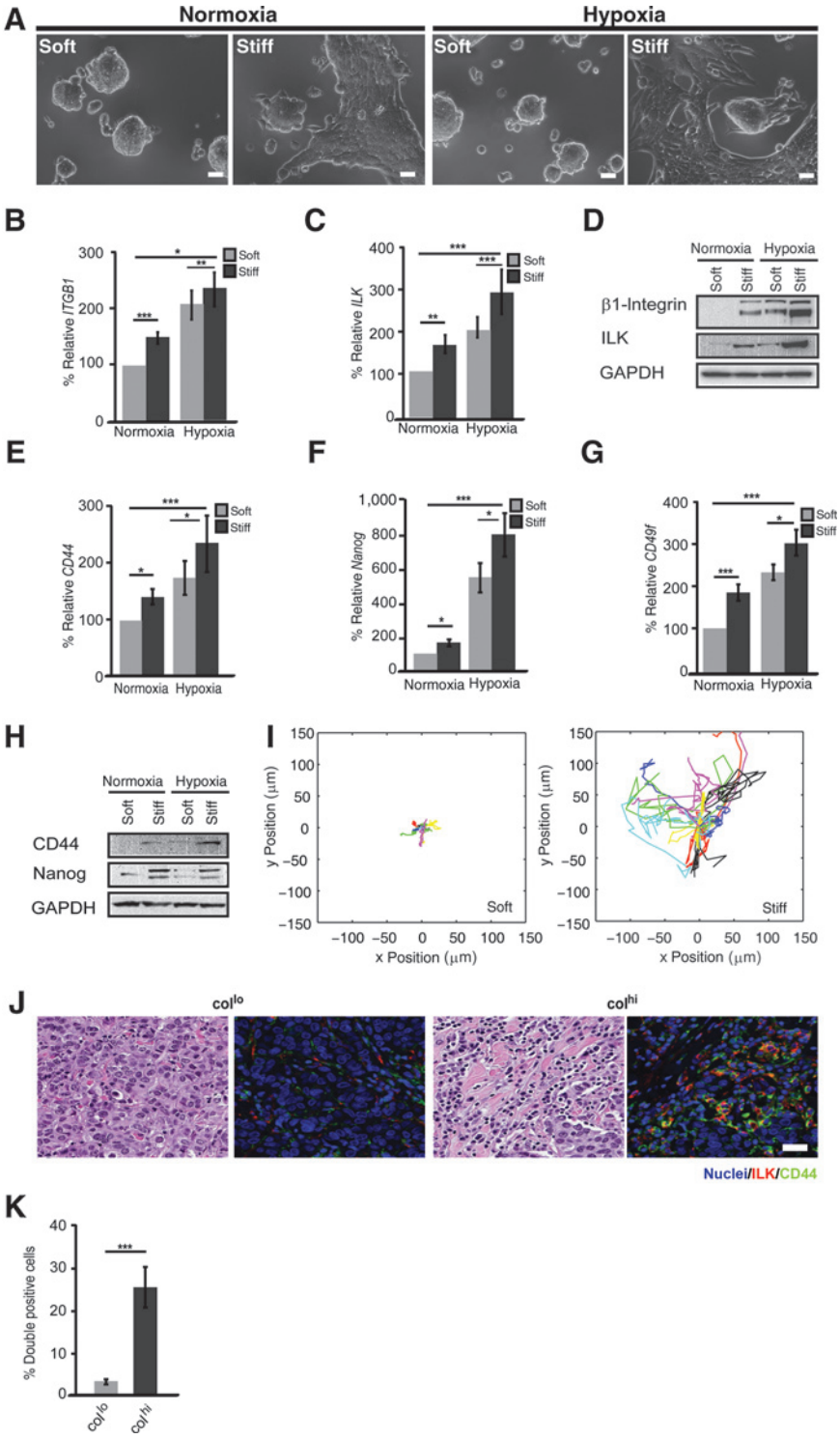

Figure 1.
Stiff and hypoxic microenvironments promote the expression of β1-integrin, ILK, and CSC markers. **A,** phase-contrast images of 4T1 mouse mammary carcinoma cells cultured on soft (E∼130 Pa) or stiff (E∼4020 Pa) polyacrylamide substrata under normoxia or hypoxia. Transcript levels of β1-integrin (*ITGB1*; **B**) and *ILK* (**C**) in 4T1 cells cultured on soft or stiff substrata under normoxia or hypoxia. **D,** immunoblotting analysis for β1-integrin and ILK in 4T1 cells cultured on soft or stiff substrata under normoxia or hypoxia. GAPDH was used as a loading control. Transcript levels of *CD44* (**E**), *Nanog* (**F**), and *CD49f* (**G**) in 4T1 cells cultured on soft or stiff substrata under normoxia or hypoxia. **H,** immunoblotting analysis for CD44 and Nanog in 4T1 cells cultured on soft or stiff substrata under normoxia or hypoxia. **I,** tracks of 4T1 cells cultured on soft or stiff substrata. **J,** IHC for ILK and CD44 in human breast cancer samples. **K,** quantification of ILK/CD44 double-positive cells in human breast cancer samples. Scale bars, 50 μm. Shown are mean ± SEM. *, $P < 0.05$; **, $P < 0.01$; ***, $P < 0.001$.

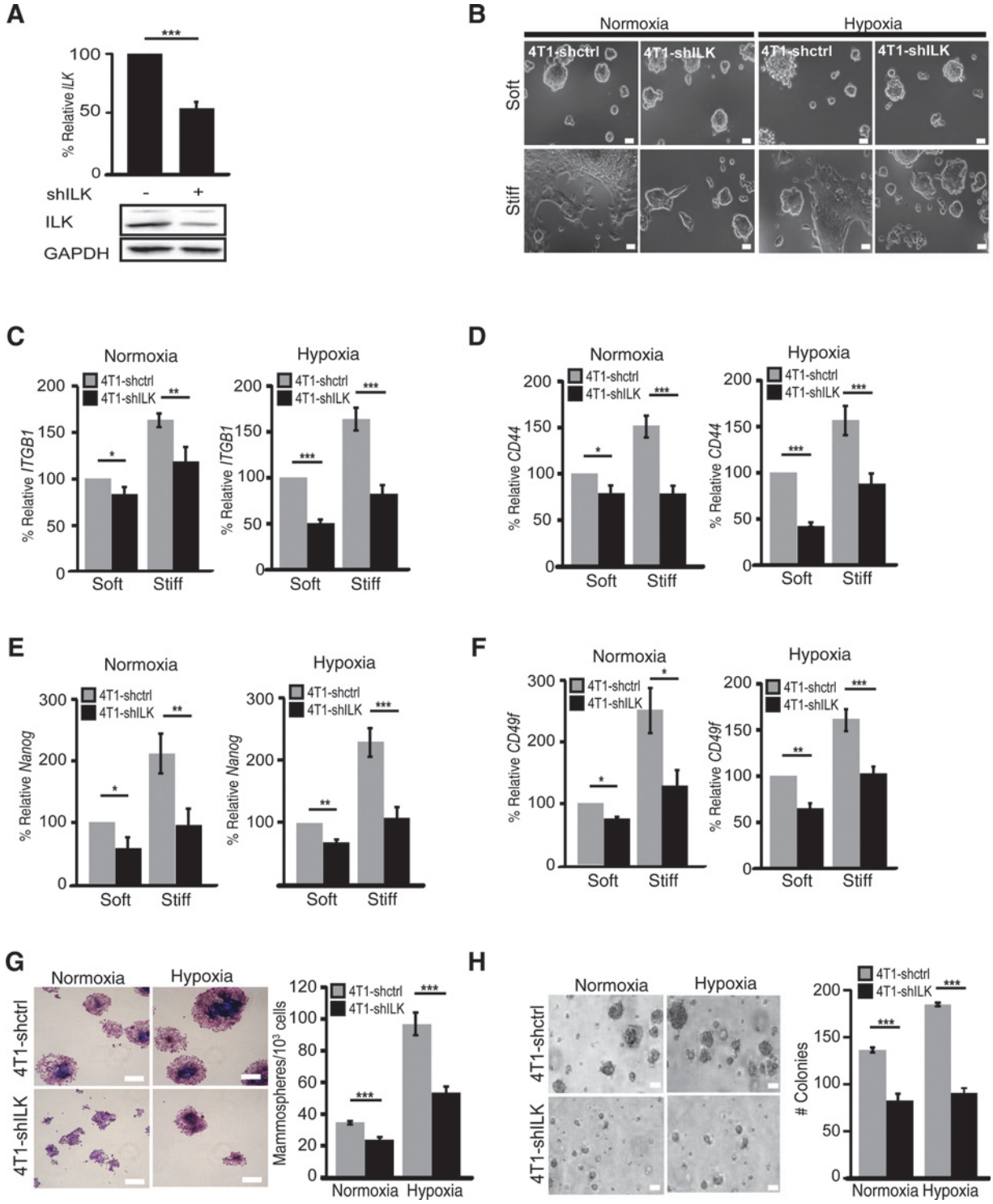

Figure 2.

ILK is required for CSC development from invasive breast cancer cells. **A,** qRT-PCR and immunoblotting analysis for ILK in 4T1 cells stably expressing shRNA against ILK (shILK) or scrambled sequence control (shctrl). **B,** phase-contrast images of 4T1-shctrl and 4T1-shILK cells cultured on soft or stiff substrata under normoxia or hypoxia. Transcript levels of *ITGB1* (**C**), *CD44* (**D**), *Nanog* (**E**), and *CD49f* (**F**) in 4T1-shctrl or 4T1-shILK cells cultured on soft or stiff substrata under normoxia or hypoxia. Phase-contrast images and quantification of secondary mammospheres (**G**) and colonies formed in soft agar (**H**) by 4T1-shctrl and 4T1-shILK cells. Scale bars, 50 μm. Shown are mean ± SEM. *, $P < 0.05$; **, $P < 0.01$; ***, $P < 0.001$.

been implicated in human cancer (23, 24). Matrix stiffness has been shown to increase integrin signaling and promote tumor progression (9). To define the role of ILK in the CSC response to stiffness and hypoxia, we used short hairpin RNA (shRNA) to stably deplete *ILK* in 4T1 (4T1-shILK) (Fig. 2A) and MDA-MB-231 cells (Supplementary Fig. S2). Depleting ILK led to a significant change in the morphology of 4T1 cells cultured on stiff substratum, as compared with scrambled controls (4T1-shctrl; Fig. 2B). On stiff substrata, 4T1-shILK cells exhibited a rounded morphology, similar to those on soft substrata, under both normoxia and hypoxia. We also found that knockdown of ILK reduced the expression of β1-integrin (Fig. 2C) and the CSC markers *CD44* (Fig. 2D), *Nanog* (Fig. 2E), and *CD49f* (Fig. 2F) in 4T1 and MDA-MB-231 cells (Supplementary Fig. S2) under both normoxia and hypoxia. To examine the role of ILK in the regulation of the CSC characteristics of anchorage-independent growth and self-renewal, we performed secondary mammosphere formation and soft agar assays. We found that depleting ILK abrogated the ability of both 4T1 and MDA-MB-231 cells to form secondary mammospheres (Fig. 2G and Supplementary Fig. S2) and colonies in soft agar (Fig. 2H; Supplementary Fig. S2). Together, these data suggest that ILK is necessary for the induction of CSC marker expression and behavior in breast cancer cells in response to matrix stiffness and hypoxia.

ILK expression enhances breast CSC development

To determine whether ILK is sufficient to induce the development of breast CSCs in the absence of a stiff microenvironment, we expressed ILK ectopically using a bicistronic recombinant adenovirus encoding for ILK and GFP (adILK). As a control, we used adenovirus encoding for GFP alone (adGFP). Transduction with adILK approximately doubled the levels of ILK transcript and protein in 4T1 (Fig. 3A) and MDA-MB-231 cells (Supplementary Fig. S3), and increased phosphorylation of Akt (pAkt; S437; Fig. 3B and Supplementary Fig. S3). qRT-PCR analysis revealed that ectopic expression of ILK increased the transcript levels of *β1-integrin* (Fig. 3C), *CD44* (Fig. 3D), *Nanog* (Fig. 3E), and *CD49f* (Fig. 3F) in 4T1 and MDA-MB-231 cells (Supplementary Fig. S3) cultured on soft or stiff substrata under normoxia or hypoxia. Ectopic expression of ILK also enhanced the formation of secondary mammospheres (Fig. 3G and Supplementary Fig. S3) and colonies in soft agar (Fig. 3H and Supplementary Fig. S3), demonstrating that increased expression of ILK can further activate CSC gene expression and behavior even when cells are cultured on stiff substrata under hypoxic conditions.

ILK signals through PI3K/Akt to regulate CSC development

Previous work has suggested that ILK regulates cell survival through the PI3K/Akt pathway (32), which has also been implicated in cancer cell (33, 34) and CSC survival (35, 36), cancer cell proliferation (37, 38), and the CSC phenotype (39). We found that knockdown of ILK reduced the phosphorylation of Akt (Fig. 4A and Supplementary Fig. S4). Disrupting signaling through PI3K by treating cells with the selective inhibitor, LY294002 (Fig. 4B and Supplementary Fig. S4), also decreased the transcript levels of *β1-integrin* (Fig. 4C) and *ILK* (Fig. 4D) in 4T1 and MDA-MB-231 cells (Supplementary Fig. S4) cultured on soft or stiff substrata under normoxia or hypoxia. Consistent with the concept that Akt activation is necessary for the ILK-dependent induction of CSCs in response to hypoxia or a stiff microenvironment, the levels of *CD44* (Fig. 4E), *Nanog* (Fig. 4F), and *CD49f* (Fig. 4G) decreased significantly in response to treatment with LY294002 in 4T1 and MDA-MB-231 cells (Supplementary Fig. S4) under all conditions.

Similarly, treatment with LY294002 reduced the formation of both secondary mammospheres (Fig. 4H) and colonies in soft agar (Fig. 4I). These data suggest that a stiff, hypoxic microenvironment regulates development of CSCs in part by activating signaling through ILK and PI3K.

Stiff substratum promotes angiogenesis and dissemination of tumor cells through ILK

To test directly whether stiff substratum promotes tumorigenesis and tumor cell dissemination, we embedded 4T1 cells in collagen gels of low (col^{lo}, 3 mg/mL), medium (col^{med}, 4.5 mg/mL), or high (col^{hi}, 6 mg/mL) stiffness (Fig. 5A) and then grafted them onto the CAMs of chicken embryos (40). We found that all col^{hi}-grafted CAMs formed primary tumors at the graft sites, whereas none of the col^{lo}- and only 4 of 6 of the col^{med}-grafted CAMs developed primary tumors (Fig. 5B). The tumors that formed in high collagen developed multiple micrometastases near blood vessels adjacent to the graft sites (Fig. 5C). To define the effects of ILK on tumor formation, we performed CAM assays using 4T1-shctrl or 4T1-shILK cells embedded in high collagen gels. Both 4T1-shctrl and 4T1-shILK cells formed primary tumors on the CAM (Fig. 5D). However, the 4T1-shILK primary tumors were half the size of the 4T1-shctrl tumors (Fig. 5D). To examine how ILK affects metastatic potential, we performed qRT-PCR analysis for *GFP* in the lungs of the chicken embryos after 5 days of incubation with GFP-labeled 4T1 cells. We found significantly lower levels of *GFP* in the lungs of embryos with 4T1-shILK-grafted CAMs than in those with 4T1-shctrl–grafted CAMs (Fig. 5E). These data suggest that matrix stiffness and ILK affect tumor formation as well as tumor cell dissemination.

Angiogenesis is a hallmark of cancer that is critical for tumor growth and metastasis (41). To investigate how substratum stiffness affects hypoxia-dependent angiogenesis, we examined the expression of VEGF-A in 4T1 cells cultured on soft or stiff substrata under normoxia or hypoxia. We found that culture on stiff substratum upregulated the expression of *VEGF-A* (Fig. 5F), suggesting that the mechanical properties of the microenvironment can regulate angiogenic signaling. As expected, hypoxia further increased the levels of *VEGF-A* in cells cultured on both soft and stiff substrata (Fig. 5F). Depleting ILK significantly reduced *VEGF-A* expression in 4T1 cells cultured on soft or stiff substrata under normoxia or hypoxia (Fig. 5G). Quantitative image analysis revealed that the blood vessel density in the CAM adjacent to 4T1-shILK tumors was significantly lower than that adjacent to 4T1-shctrl tumors (Fig. 5H). These data suggest that loss of ILK impairs the angiogenic potential of breast cancer cells. Consistently, we found that inhibiting PI3K with LY294002 significantly reduced the levels of *VEGF-A* (Fig. 5I), whereas ectopic expression of ILK increased the levels of *VEGF-A* (Fig. 5J) under all culture conditions. These data suggest that ILK signals through the PI3K pathway to regulate VEGF-A expression in response to matrix stiffness and hypoxia.

Discussion

It is well appreciated that the distinct physical properties of the tumor microenvironment can affect cancer cell fate. Tumor stiffness induces integrin clustering and downstream signaling that control cancer cell proliferation, gene expression, and

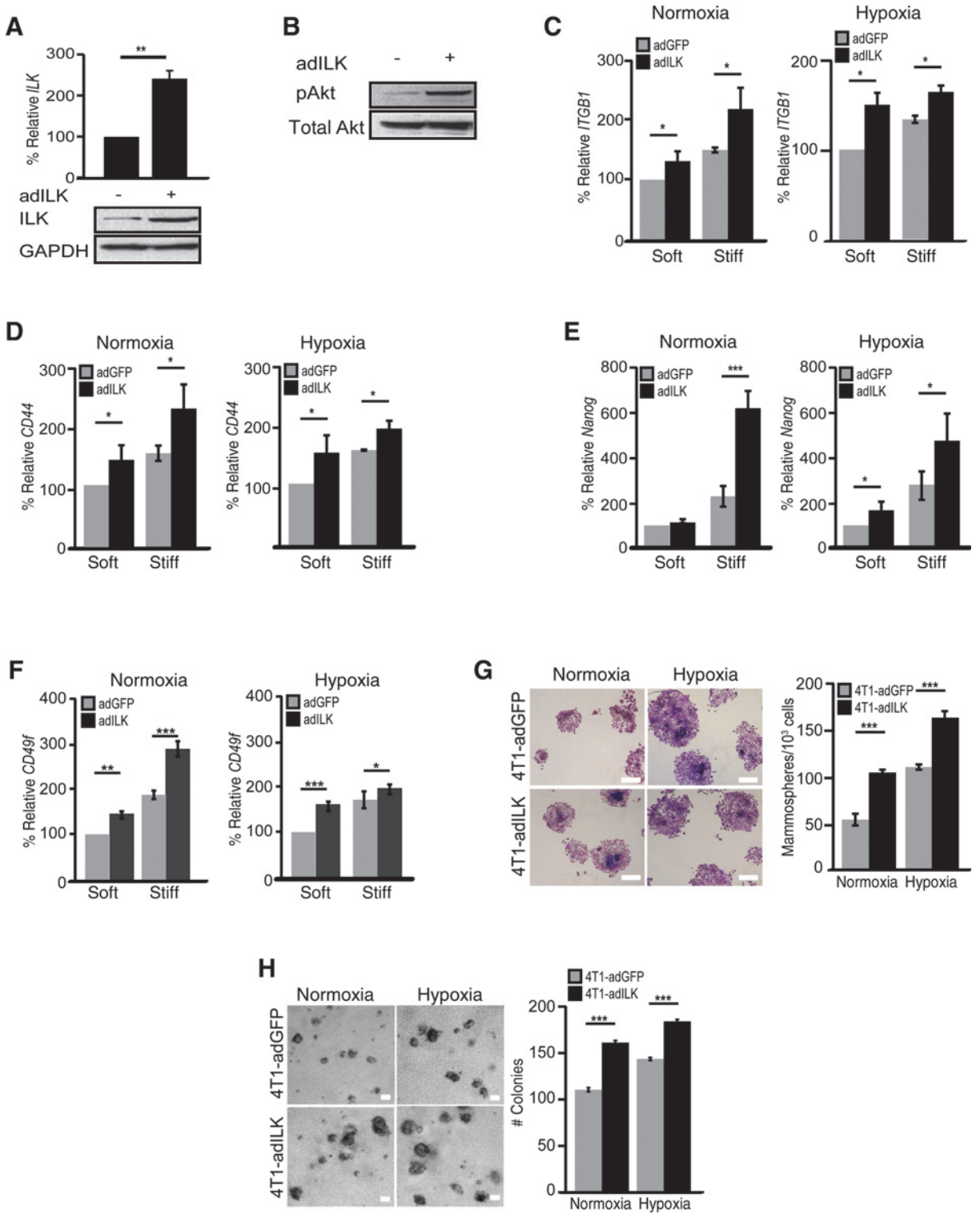

Figure 3.

Ectopic expression of ILK induces breast CSCs. **A,** qRT-PCR and immunoblotting analysis for ILK in 4T1 cells transduced with adGFP or adILK. **B,** immunoblotting analysis for phosphorylated and total Akt in 4T1 cells transduced with adGFP or adILK. Transcript levels of *ITGB1* (**C**), *CD44* (**D**), *Nanog* (**E**), and *CD49f* (**F**) in 4T1 cells transduced with adGFP or adILK cultured on soft or stiff substrata under normoxia or hypoxia. Phase-contrast images and quantification of secondary mammospheres (**G**) and colonies formed in soft agar (**H**) by 4T1 cells transduced with adGFP or adILK. Scale bars, 50 μm. Shown are mean ± SEM. *, $P < 0.05$; **, $P < 0.01$; ***, $P < 0.001$.

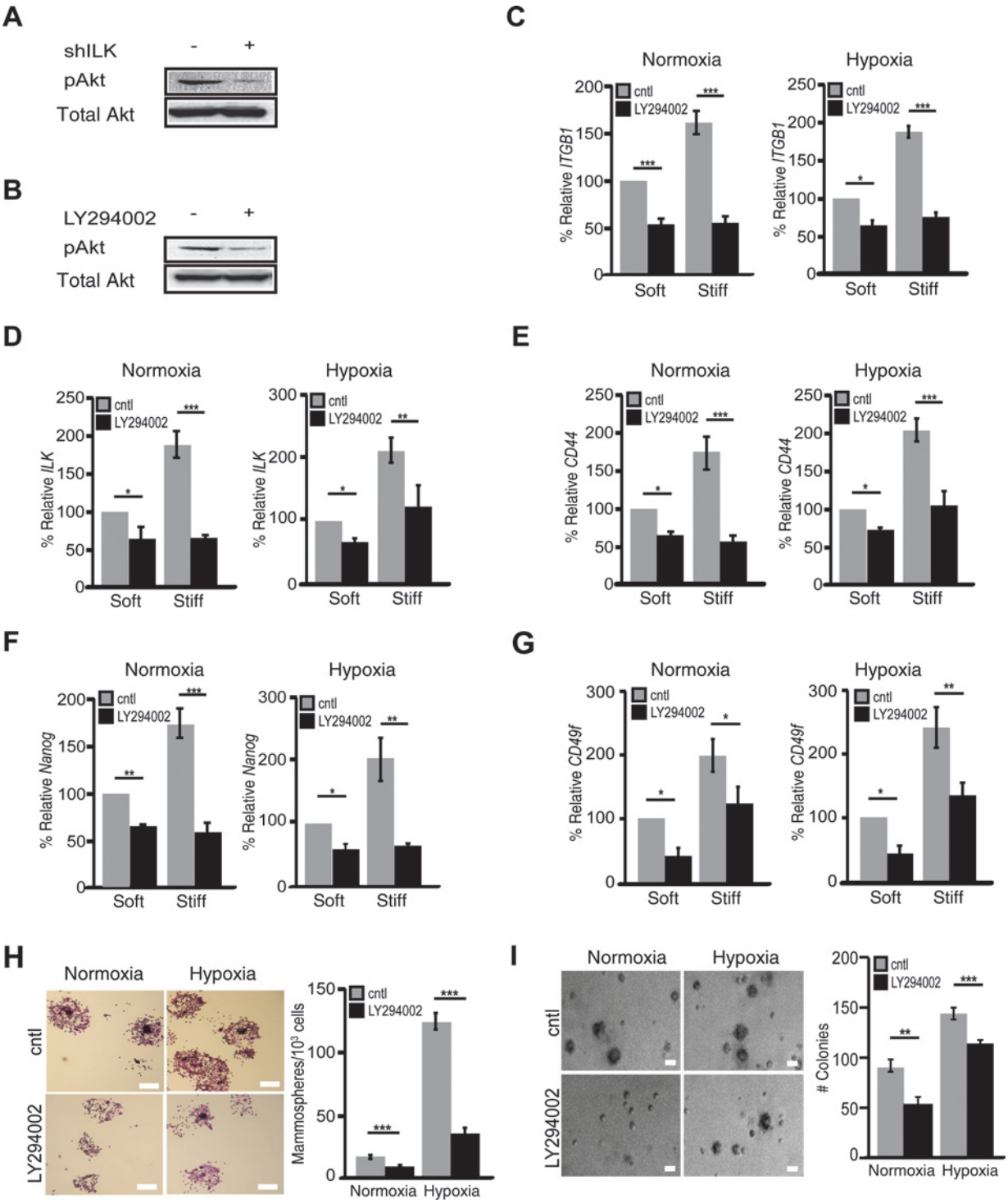

Figure 4.

ILK induces breast CSCs by signaling through PI3K. Immunoblotting analysis for phosphorylated and total Akt in 4T1-shctrl and 4T1-shILK cells (**A**) or 4T1 cells treated with or without LY294002 (50 μmol/L; **B**). Transcript levels of *ITGB1* (**C**), *ILK* (**D**), *CD44* (**E**), *Nanog* (**F**), and *CD49f* (**G**) in 4T1 cells treated with or without LY294002 cultured on soft or stiff substrata under normoxia or hypoxia. Phase-contrast images and quantification of secondary mammospheres (**H**) and colonies formed in soft agar (**I**) by 4T1 cells treated with or without LY294002 under normoxia or hypoxia. Scale bars, 50 μm. Shown are mean ± SEM. *, $P < 0.05$; **, $P < 0.01$; ***, $P < 0.001$.

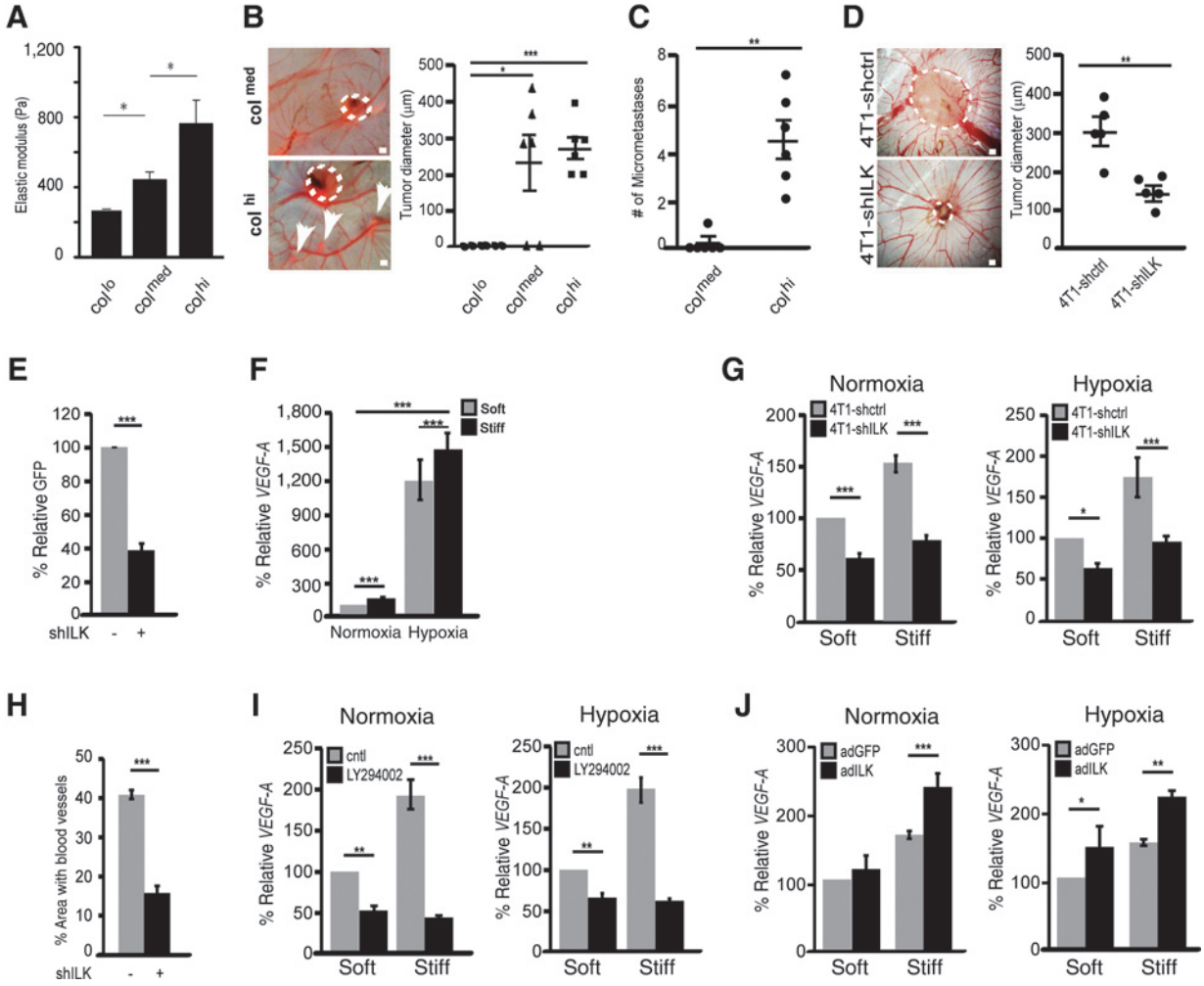

Figure 5.

Stiff substratum and ILK signaling promote tumor growth, angiogenesis, and metastasis. **A,** estimated elastic modulus of low, medium, and high concentration collagen gels. Brightfield images and quantification of tumor diameter (**B**) and number of micrometastases (**C**) formed by 4T1 cells embedded in low, medium, or high concentrations of collagen implanted on CAMs. Scale bars, 50 μm. **D,** representative images and quantification of tumor diameter on CAMs grafted with 4T1-shctrl and 4T1-shILK cells. Scale bars, 25 μm. **E,** transcript levels of *GFP* in the lungs of chicken embryos whose CAMs were grafted with 4T1-shctrl or 4T1-shILK cells. Transcript levels of *VEGF-A* in 4T1 cells (**F**) or 4T1-shctrl and 4T1-shILK cells (**G**) cultured on soft or stiff substrata under normoxia or hypoxia. **H,** quantification of the relative area of the CAM covered with blood vessels 5 days after grafting with 4T1-shctrl or 4T1-shILK cells. Transcript levels of *VEGF-A* in 4T1 cells treated with or without LY294002 (**I**) or transduced with adGFP or adILK (**J**) and cultured on soft or stiff substrata under normoxia or hypoxia. Shown are mean ± SEM. *, $P < 0.05$; **, $P < 0.01$; ***, $P < 0.001$.

invasiveness (8, 42, 43). Separately, hypoxia promotes CSC properties, in part through activation of hypoxia-inducible factors (HIFs) that regulate the expression of stem cell markers (16, 44). Here, we found that these two features of the tumor microenvironment, hypoxia and substratum stiffness, work synergistically through ILK to enhance breast CSC gene expression, tumor growth, and metastasis. Future work using limiting dilution assays *in vivo* with cells primed by hypoxia, stiff substrata, and/or ILK might clarify which subpopulation has the highest tumor-initiating potential, but experimental approaches that maintain the microenvironmental conditions of the injected cells need to be developed. Nonetheless, our findings are congruent with clinical data showing that hypoxia and stiffness correlate with a poor prognosis in breast cancer (45, 46).

Also known as tumor-repopulating cells or tumor-initiating cells, CSCs represent a self-renewing subpopulation of cancer cells that promote tumor progression of many solid cancers, including those of the breast, colon, and brain (47). While our data suggest that stiff and hypoxic microenvironments promote the development of CSCs from breast cancer cells, this relationship is probably not generalizable to all tumor types and stages. Indeed, melanoma tumor-repopulating cells preferentially self-renew on soft substrata in a Sox2-dependent manner (48). In contrast, glioblastoma tumor-initiating cells are insensitive to matrix mechanics, and enhancing their cytoskeletal contractility causes a loss of their tumor-promoting properties (49). In the breast, mechanosensing and mechanotransduction are altered as a function of aging (50), so the effects of stiffness on CSCs likely also depends on age.

Matrix stiffness clearly activates signaling through β1-integrin, which transmits information about the mechanical properties of the microenvironment through the ILK/PI3K/Akt pathway and eventually to CSC-related genes, including the CSC markers examined here – CD44, Nanog, CD49f, and ALDH. ILK is well appreciated for its roles in stemness and metastasis (33, 34, 37) and is known to stimulate tumor angiogenesis through VEGF-A (51). Our data suggest a positive feedback loop in which the signaling activated by ILK induces increased expression of mechanosensors, including β1-integrin and ILK itself. Hypoxia enhances activation of this mechanotransduction pathway, and while the exact mechanism by which this occurs is not clear, hypoxia has been found to upregulate the expression of ILK in prostate cancer (52) and colorectal cancer cells (53) in a HIF1α-dependent manner (54). Recent studies indicate that HIF1α can drive breast cancer metastasis through ECM stiffening and collagen fiber alignment (55). It is possible that hypoxia promotes ECM remodeling and, concomitantly, elevates the levels of ILK to prime breast cancer cells to be more sensitive to mechanically stiff microenvironments. Our results clearly indicate that loss of ILK abrogates the mechanosensing capability of tumor cells, prevents the development of CSCs, and blocks tumor growth and dissemination. These data suggest that ILK acts as a critical mechanosensor that signals through the PI3K/Akt pathway to mediate the formation of breast CSCs under stiff and hypoxic conditions. The stiff, hypoxic regions of a tumor might, therefore, be responsible for inducing both CSC gene expression and behavior in tumor cells residing within, as well as angiogenesis to facilitate tumor cell dissemination. Therapies targeted at microenvironment-induced signaling would need to address both physical properties to disrupt the formation and metastatic spread of breast CSCs.

Disclosure of Potential Conflicts of Interest

No potential conflicts of interest were disclosed.

Authors' Contributions

Conception and design: M.-F. Pang, D.C. Radisky, C.M. Nelson
Development of methodology: M.-F. Pang, S. Han
Acquisition of data (provided animals, acquired and managed patients, provided facilities, etc.): M.-F. Pang, M.J. Siedlik, S. Han, M. Stallings-Mann
Analysis and interpretation of data (e.g., statistical analysis, biostatistics, computational analysis): M.-F. Pang, M.J. Siedlik, S. Han, M. Stallings-Mann
Writing, review, and/or revision of the manuscript: M.-F. Pang, M.J. Siedlik, D.C. Radisky, C.M. Nelson
Study supervision: C.M. Nelson

Acknowledgments

We thank Christina J. DeCoste and John J. Grady for their technical support with flow cytometry.

Grant Support

This work was supported in part by grants from the NIH (GM083997, HL110335, HL118532, HL120142), the NSF (CMMI-1435853), the David & Lucile Packard Foundation, the Alfred P. Sloan Foundation, the Camille & Henry Dreyfus Foundation, and the Burroughs Wellcome Fund (C.M. Nelson), and by a grant from the NIH (CA187692 to C.M. Nelson and D.C. Radisky). M.-F. Pang was supported in part by postdoctoral fellowships from the Swedish Society for Medical Research (SSMF) and the New Jersey Commission on Cancer Research (NJCCR). M. J. Siedlik was supported in part by the NSF Graduate Research Fellowship program.

The costs of publication of this article were defrayed in part by the payment of page charges. This article must therefore be hereby marked *advertisement* in accordance with 18 U.S.C. Section 1734 solely to indicate this fact.

Received March 1, 2016; revised July 14, 2016; accepted July 15, 2016; published OnlineFirst August 8, 2016.

References

1. Engler AJ, Sen S, Sweeney HL, Discher DE. Matrix elasticity directs stem cell lineage specification. Cell 2006;126:677–89.
2. Butcher DT, Alliston T, Weaver VM. A tense situation: forcing tumour progression. Nat Rev Cancer 2009;9:108–22.
3. Lui C, Lee K, Nelson CM. Matrix compliance and RhoA direct the differentiation of mammary progenitor cells. Biomech Model Mechanobiol 2012;11:1241–9.
4. Lee K, Chen QK, Lui C, Cichon MA, Radisky DC, Nelson CM. Matrix compliance regulates Rac1b localization, NADPH oxidase assembly, and epithelial-mesenchymal transition. Mol Biol Cell 2012;23:4097–108.
5. Boyd NF, Rommens JM, Vogt K, Lee V, Hopper JL, Yaffe MJ, et al. Mammographic breast density as an intermediate phenotype for breast cancer. Lancet Oncol 2005;6:798–808.
6. Li T, Sun L, Miller N, Nicklee T, Woo J, Hulse-Smith L, et al. The association of measured breast tissue characteristics with mammographic density and other risk factors for breast cancer. Cancer Epidemiol Biomarkers Prev 2005;14:343–9.
7. Paszek MJ, Zahir N, Johnson KR, Lakins JN, Rozenberg GI, Gefen A, et al. Tensional homeostasis and the malignant phenotype. Cancer Cell 2005;8:241–54.
8. Goetz JG, Minguet S, Navarro-Lerida I, Lazcano JJ, Samaniego R, Calvo E, et al. Biomechanical remodeling of the microenvironment by stromal caveolin-1 favors tumor invasion and metastasis. Cell 2011;146:148–63.
9. Levental KR, Yu H, Kass L, Lakins JN, Egeblad M, Erler JT, et al. Matrix crosslinking forces tumor progression by enhancing integrin signaling. Cell 2009;139:891–906.
10. Axelson H, Fredlund E, Ovenberger M, Landberg G, Pahlman S. Hypoxia-induced dedifferentiation of tumor cells–a mechanism behind heterogeneity and aggressiveness of solid tumors. Semin Cell Dev Biol 2005;16:554–63.
11. Bos R, Zhong H, Hanrahan CF, Mommers EC, Semenza GL, Pinedo HM, et al. Levels of hypoxia-inducible factor-1 alpha during breast carcinogenesis. J Natl Cancer Inst 2001;93:309–14.
12. Zhong H, De Marzo AM, Laughner E, Lim M, Hilton DA, Zagzag D, et al. Overexpression of hypoxia-inducible factor 1alpha in common human cancers and their metastases. Cancer Res 1999;59:5830–5.
13. Miller KD. E2100: a phase III trial of paclitaxel versus paclitaxel/bevacizumab for metastatic breast cancer. Clin Breast Cancer 2003;3:421–2.
14. Valent P, Bonnet D, De Maria R, Lapidot T, Copland M, Melo JV, et al. Cancer stem cell definitions and terminology: the devil is in the details. Nat Rev Cancer 2012;12:767–75.
15. Xing F, Okuda H, Watabe M, Kobayashi A, Pai SK, Liu W, et al. Hypoxia-induced Jagged2 promotes breast cancer metastasis and self-renewal of cancer stem-like cells. Oncogene 2011;30:4075–86.
16. Mathieu J, Zhang Z, Zhou W, Wang AJ, Heddleston JM, Pinna CM, et al. HIF induces human embryonic stem cell markers in cancer cells. Cancer Res 2011;71:4640–52.
17. Louie E, Nik S, Chen JS, Schmidt M, Song B, Pacson C, et al. Identification of a stem-like cell population by exposing metastatic breast cancer cell lines to repetitive cycles of hypoxia and reoxygenation. Breast Cancer Res 2010;12:R94.
18. Al-Hajj M, Wicha MS, Benito-Hernandez A, Morrison SJ, Clarke MF. Prospective identification of tumorigenic breast cancer cells. Proc Natl Acad Sci U S A 2003;100:3983–8.
19. Velasco-Velazquez MA, Homsi N, De La Fuente M, Pestell RG. Breast cancer stem cells. Int J Biochem Cell Biol 2012;44:573–7.
20. Koh MY, Powis G. Passing the baton: the HIF switch. Trends Biochem Sci 2012;37:364–72.
21. Yoshida Y, Takahashi K, Okita K, Ichisaka T, Yamanaka S. Hypoxia enhances the generation of induced pluripotent stem cells. Cell Stem Cell 2009;5:237–41.

22. Hannigan G, Troussard AA, Dedhar S. Integrin-linked kinase: a cancer therapeutic target unique among its ILK. Nat Rev Cancer 2005;5: 51–63.
23. Graff JR, Deddens JA, Konicek BW, Colligan BM, Hurst BM, Carter HW, et al. Integrin-linked kinase expression increases with prostate tumor grade. Clin Cancer Res 2001;7:1987–91.
24. Ito R, Oue N, Zhu X, Yoshida K, Nakayama H, Yokozaki H, et al. Expression of integrin-linked kinase is closely correlated with invasion and metastasis of gastric carcinoma. Virchows Arch 2003;442:118–23.
25. Chan J, Ko FC, Yeung YS, Ng IO, Yam JW. Integrin-linked kinase overexpression and its oncogenic role in promoting tumorigenicity of hepatocellular carcinoma. PLoS One 2011;6:e16984.
26. Varner VD, Gleghorn JP, Miller E, Radisky DC, Nelson CM. Mechanically patterning the embryonic airway epithelium. Proc Natl Acad Sci U S A 2015;112:9230–5.
27. Palmer TD, Lewis J, Zijlstra A. Quantitative analysis of cancer metastasis using an avian embryo model. J Vis Exp 2011;51:e2815.
28. Favaro E, Lord S, Harris AL, Buffa FM. Gene expression and hypoxia in breast cancer. Genome Med 2011;3:55.
29. Velasco-Velazquez MA, Popov VM, Lisanti MP, Pestell RG. The role of breast cancer stem cells in metastasis and therapeutic implications. Am J Pathol 2011;179:2–11.
30. Cox TR, Erler JT. Remodeling and homeostasis of the extracellular matrix: implications for fibrotic diseases and cancer. Dis Model Mech 2011;4:165–78.
31. Fenner J, Stacer AC, Winterroth F, Johnson TD, Luker KE, Luker GD. Macroscopic stiffness of breast tumors predicts metastasis. Sci Rep 2014;4: 5512.
32. Nho RS, Xia H, Kahm J, Kleidon J, Diebold D, Henke CA. Role of integrin-linked kinase in regulating phosphorylation of Akt and fibroblast survival in type I collagen matrices through a beta1 integrin viability signaling pathway. J Biol Chem 2005;280:26630–9.
33. Garcia-Regalado A, Vargas M, Garcia-Carranca A, Arechaga-Ocampo E, Gonzalez-De la Rosa CH. Activation of Akt pathway by transcription-independent mechanisms of retinoic acid promotes survival and invasion in lung cancer cells. Mol Cancer 2013;12:44.
34. Clark AS, West K, Streicher S, Dennis PA. Constitutive and inducible Akt activity promotes resistance to chemotherapy, trastuzumab, or tamoxifen in breast cancer cells. Mol Cancer Ther 2002;1:707–17.
35. Hambardzumyan D, Becher OJ, Rosenblum MK, Pandolfi PP, Manova-Todorova K, Holland EC. PI3K pathway regulates survival of cancer stem cells residing in the perivascular niche following radiation in medulloblastoma in vivo. Genes Dev 2008;22:436–48.
36. Dubrovska A, Kim S, Salamone RJ, Walker JR, Maira SM, Garcia-Echeverria C, et al. The role of PTEN/Akt/PI3K signaling in the maintenance and viability of prostate cancer stem-like cell populations. Proc Natl Acad Sci U S A 2009;106:268–73.
37. Yang XL, Lin FJ, Guo YJ, Shao ZM, Ou ZL. Gemcitabine resistance in breast cancer cells regulated by PI3K/AKT-mediated cellular proliferation exerts negative feedback via the MEK/MAPK and mTOR pathways. Onco Targets Ther 2014;7:1033–42.
38. Li X, Kong X, Wang Y, Yang Q. BRCC2 inhibits breast cancer cell growth and metastasis in vitro and in vivo via downregulating AKT pathway. Cell Death Dis 2013;4:e757.
39. Bleau AM, Hambardzumyan D, Ozawa T, Fomchenko EI, Huse JT, Brennan CW, et al. PTEN/PI3K/Akt pathway regulates the side population phenotype and ABCG2 activity in glioma tumor stem-like cells. Cell Stem Cell 2009;4:226–35.
40. Lokman NA, Elder AS, Ricciardelli C, Oehler MK. Chick chorioallantoic membrane (CAM) assay as an in vivo model to study the effect of newly identified molecules on ovarian cancer invasion and metastasis. Int J Mol Sci 2012;13:9959–70.
41. Weis SM, Cheresh DA. Tumor angiogenesis: molecular pathways and therapeutic targets. Nat Med 2011;17:1359–70.
42. Provenzano PP, Inman DR, Eliceiri KW, Knittel JG, Yan L, Rueden CT, et al. Collagen density promotes mammary tumor initiation and progression. BMC Med 2008;6:11.
43. Paszek MJ, Weaver VM. The tension mounts: mechanics meets morphogenesis and malignancy. J Mammary Gland Biol Neoplasia 2004; 9:325–42.
44. Xiang L, Gilkes DM, Hu H, Takano N, Luo W, Lu H, et al. Hypoxia-inducible factor 1 mediates TAZ expression and nuclear localization to induce the breast cancer stem cell phenotype. Oncotarget 2014;5: 12509–27.
45. Schindl M, Schoppmann SF, Samonigg H, Hausmaninger H, Kwasny W, Gnant M, et al. Overexpression of hypoxia-inducible factor 1alpha is associated with an unfavorable prognosis in lymph node-positive breast cancer. Clin Cancer Res 2002;8:1831–7.
46. Wei SC, Fattet L, Tsai JH, Guo Y, Pai VH, Majeski HE, et al. Matrix stiffness drives epithelial-mesenchymal transition and tumour metastasis through a TWIST1-G3BP2 mechanotransduction pathway. Nat Cell Biol 2015;17: 678–88.
47. Reya T, Morrison SJ, Clarke MF, Weissman IL. Stem cells, cancer, and cancer stem cells. Nature 2001;414:105–11.
48. Tan Y, Tajik A, Chen J, Jia Q, Chowdhury F, Wang L, et al. Matrix softness regulates plasticity of tumour-repopulating cells via H3K9 demethylation and Sox2 expression. Nat Commun 2014;5:4619.
49. Wong SY, Ulrich TA, Deleyrolle LP, MacKay JL, Lin JM, Martuscello RT, et al. Constitutive activation of myosin-dependent contractility sensitizes glioma tumor-initiating cells to mechanical inputs and reduces tissue invasion. Cancer Res 2015;75:1113–22.
50. Pelissier FA, Garbe JC, Ananthanarayanan B, Miyano M, Lin C, Jokela T, et al. Age-related dysfunction in mechanotransduction impairs differentiation of human mammary epithelial progenitors. Cell Rep 2014;7: 1926–39.
51. Tan C, Cruet-Hennequart S, Troussard A, Fazli L, Costello P, Sutton K, et al. Regulation of tumor angiogenesis by integrin-linked kinase (ILK). Cancer Cell 2004;5:79–90.
52. Chou CC, Chuang HC, Salunke SB, Kulp SK, Chen CS. A novel HIF-1alpha-integrin-linked kinase regulatory loop that facilitates hypoxia-induced HIF-1alpha expression and epithelial-mesenchymal transition in cancer cells. Oncotarget 2015;6:8271–85.
53. Xiao L, Yue X, Ming X, Xu L, Ding M, Xu J, et al. The integrin-linked kinase gene up-regulated by hypoxia plays its pro-survival role in colorectal cancer cells. J Recept Signal Transduct Res 2014;34:64–72.
54. Abboud ER, Coffelt SB, Figueroa YG, Zwezdaryk KJ, Nelson AB, Sullivan DE, et al. Integrin-linked kinase: a hypoxia-induced anti-apoptotic factor exploited by cancer cells. Int J Oncol 2007;30:113–22.
55. Gilkes DM, Bajpai S, Chaturvedi P, Wirtz D, Semenza GL. Hypoxia-inducible factor 1 (HIF-1) promotes extracellular matrix remodeling under hypoxic conditions by inducing P4HA1, P4HA2, and PLOD2 expression in fibroblasts. J Biol Chem 2013;288:10819–29.